Proceedings of the Fifth Workshop on
Mathematical Modelling
of Environmental and Life Sciences Problems
Constanţa, Romania, September, 2006, pp. 173–180

On some constraining strategies in image reconstruction from projections

Constantin Popa[*♮] and **Rafal Zdunek**[**]

In image reconstruction from projections in computerized tomography we usually get rank-deficient linear least squares problems. This causes a blurring effect in the reconstructed image, due to the component (of the exact image) which belongs to the nonzero null space of the system matrix. In order to eliminate these unpleasant aspects, some constraining strategies have been proposed in 1990, by I. Koltracht and P. Lancaster for the classical Kaczmarz projection method. In the present paper we extend and analyse the behaviour of such constraints for the Extended Kaczmarz algorithm previously proposed by one of the authors. The numerical results are presented for some experiments associated with a "well-to-well" geometry in electromagnetic geotomography.

1. The constrained Kaczmarz algorithm

Electromagnetic geotomography (EG, for short) uses a well-to-well scanning procedure (see e.g. [5, 8]). As shown in Fig. 1(left) the electromagnetic scanning is between the boreholes. We assume several positions ($S_1, \ldots, S_p$ on AB) of an electromagnetic wave source (transmitter) in one borehole and several positions ($R_1, \ldots, R_q$ on CD) of field measurement (receiver) located in the other borehole. Then, the total number of the transmitter-receiver pairs, which is $m = pq$, becomes the number of rows in the system matrix A. Its number of columns, n is given by discretization of the scanned area as shown in Fig. 1(right). The matrix coefficient A_{ij} will be defined as the length of the intersection between the i-th ray of the electromagnetic wave with the j-th pixel, whereas the i-th component of the right hand side b_i is computed us-

[*] "Ovidius" University of Constanţa, Romania, e-mail: cpopa@univ-ovidius.ro
[**] Wroclaw University of Technology, Wroclaw, Poland, e-mail: Rafal.Zdunek@pwr.wroc.pl
[♮] The paper was supported by the Grant CEEX 05-D11-25/2005.

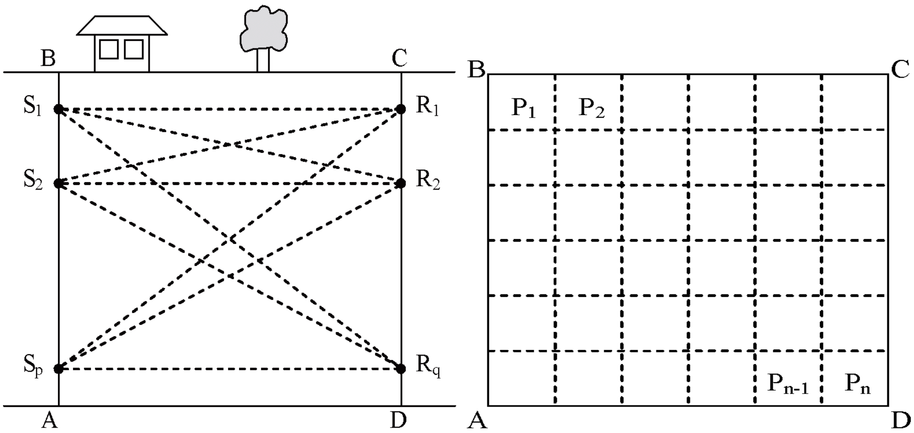

Fig. 1. (Left) Measurement setup in electromagnetic geotomography; (Right) Discretization of the scanned area.

ing the measured values of electromagnetic wave strength between the source and its receiver (see for details [5, 7, 8]). In this way we obtain the least squares formulation of the EG problem: find $x \in \mathbb{R}^n$ such that

$$\| Ax - b \| = \min!, \tag{1}$$

where A is large, sparse (because both values of m and n must be enough big for a good data acquisition) and rank-deficient (i.e. its null space, $N(A)$ is not trivial, see [4]). Moreover, because of the measurement errors, the problem (1) is also inconsistent. According to the mathematical model (1), the exact images that we are looking for are vectors, $x^{ex} = (x_1^{ex}, \ldots, x_n^{ex})^{\mathrm{T}} \in \mathbb{R}^n$ with $x_i^{ex} \in [0,1]$ (w.r.t. a gray scale, see [7]). If $LSS(A; b)$ is the set of all solutions from (1), x_{LS} is the minimal norm one and $P_S x$ is the orthogonal projection onto a vector subspace $S \subset \mathbb{R}^q$, we know that (see also Fig. 2 and [1])

$$x^{ex} = P_{N(A)} x^{ex} + x_{LS},$$

thus

$$x_{LS} = x^{ex} - P_{N(A)} x^{ex} \notin [0,1]^n, \tag{2}$$

because of the contribution of $P_{N(A)} x^{ex}$. An example in this idea is given in Fig. 3 with the simulation on a 30×30 pixels image scanned with 30×30 rays, and x_{LS} computed with the classical Kaczmarz algorithm from below.

Kaczmarz algorithm (K): let $x^0 \in \mathbb{R}^n$; for $k = 0, 1, \ldots$ do

$$x^{k+1} = K(\omega; b; x^k), \tag{3}$$

with

$$K(\omega; b; x^k) = f_1 \circ \ldots \circ f_m(\omega; b; x^k), \;\; f_i(\omega; b; x^k) = x - \omega \frac{\langle x^k, A_i \rangle - b_i}{\| A_i \|^2} A_i, \tag{4}$$

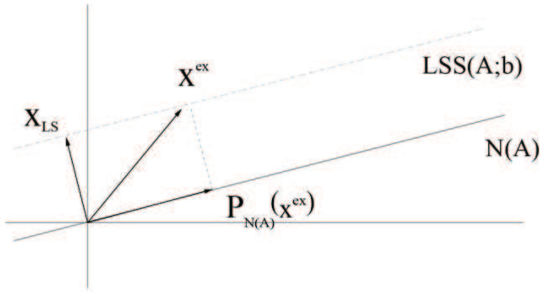

Fig. 2. Decomposition of the exact solution.

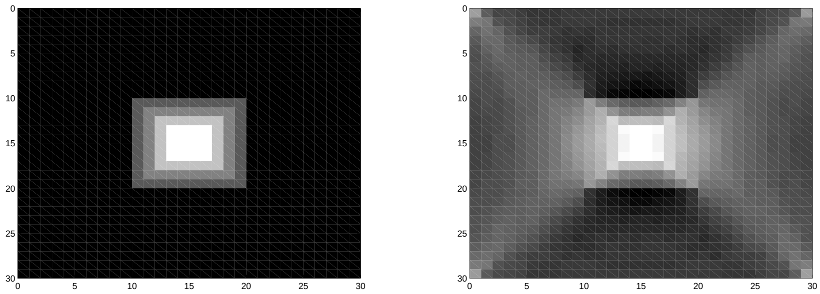

Fig. 3. (Left) Original image; (Right) Estimated image with the classical Kaczmarz algorithm.

where $A_i \neq 0$ is the i-th row of A.

Theorem 1. ([2]) *For any $x^0 \in \mathbb{R}^n$ and $\omega \in (0,2)$ the sequence $(x^k)_{k\geq 0}$ generated by the above algorithm K converges and*

$$\lim_{k\to\infty} x^k = P_{N(A)}x^0 + x_{LS} + \delta \tag{5}$$

with

$$\delta = GP_{N(A^\top)}b \tag{6}$$

and G an $n \times m$ generalized inverse of A. Moreover, if (1) *is consistent, i.e.*

$$b \in R(A), \tag{7}$$

where $R(A)$ is the range of A, then $\delta = 0$ and

$$\lim_{k\to\infty} x^k \in S(A;b), \tag{8}$$

with $\lim_{k\to\infty} x^k = x_{LS}$ if $x^0 = 0$ and $S(A;b)$ is the set of all solutions from (1) *in the consistent case* (7).

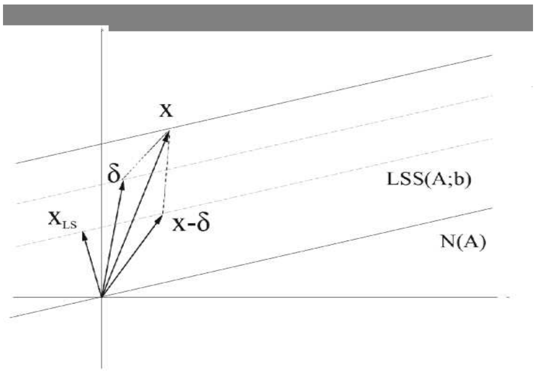

Fig. 4. Constrained Kaczmarz algorithm.

In order to eliminate the unpleased aspect from (2), a constraining procedure has been proposed in [2]. Following this, after each step of the Kaczmarz's iteration (3), the current approximation is "forced" to remain inside the interval $[0, 1]$, i.e.

$$(Cx^k)_i = \begin{cases} x_i^k, & \text{if } x_i^k \in [0,1] \\ 0, & \text{if } x_i^k < 0, \\ 1, & \text{if } x_i^k > 1. \end{cases} \tag{9}$$

In this way we obtain the Constrained Kaczmarz algorithm (CK) from below.
CK algorithm: let $x^0 \in \mathbb{R}^n$; for $k = 0, 1, \dots$ do

$$x^{k+1} = C(K(\omega; b; x^k)). \tag{10}$$

Theorem 2. ([3]) *For any $x^0 \in \mathbb{R}^n$ and $\omega \in (0, 2)$, if $(x^k)_{k \geq 0}$ is the sequence generated by the above algorithm CK, it exists $\lim_{k\to\infty} x^k = x^*$ and it satisfies:*
(i) $x^* \in [0, 1]^n$;
(ii) $x^* - \delta \in LSS(A; b)$;
(iii) *If* (7) *holds, then* $x^* \in S(A; b)$.

Remark 1. *The bigger is δ from* (6)*, the bigger will be the Euclidean distance from $x \in [0, 1]^n$ to $LSS(A; b)$* (*see also Figure* 4).

2. The constrained Kaczmarz Extended algorithm

In [6] one of the authors proposed the following extended version of the algorithm (K).

Algorithm KERP: let $x^0 \in \mathbb{R}^n$; $y^0 = b$; for $k = 0, 1, \ldots$ do

$$\begin{array}{rcl} y^{k+1} & = & (\varphi_1 \circ \ldots \circ \varphi_n)(\alpha; y^k), \\ b^{k+1} & = & b - y^{k+1}, \\ x^{k+1} & = & (f_1 \circ \ldots \circ f_m)(\omega; b^{k+1}; x^k), \end{array} \tag{11}$$

with

$$\varphi_j(\alpha; y) = y - \alpha \cdot \frac{\langle y, A^j \rangle}{\|A^j\|^2} A^j, \tag{12}$$

where $A^j \neq 0$ is the j-th column of A.

Theorem 3. ([6]) *For $x^0 = 0$ and any $\alpha, \omega \in (0, 2)$, the sequence $(x^k)_{k \geq 0}$ generated by the above algorithm KERP converges and $\lim_{k \to \infty} x^k = x_{LS}$.*

In a similar way as in Section 1 we consider the following constrained version of the above algorithm KERP.

Algorithm CKERP: let $x^0 \in \mathbb{R}^n$; $y^0 = b$; for $k = 0, 1, \ldots$ do

$$\begin{array}{rcl} y^{k+1} & = & (\varphi_1 \circ \ldots \circ \varphi_n)(\alpha; y^k), \\ b^{k+1} & = & b - y^{k+1}, \\ x^{k+1} & = & C\left[(f_1 \circ \ldots \circ f_m)(\omega; b^{k+1}; x^k)\right]. \end{array} \tag{13}$$

We conjecture the following result confirmed by the numerical experiments and the heuristic arguments from below.

Theorem 4 (conjecture**).** *For any $x^0 \in \mathbb{R}^n$, any $\alpha, \omega \in (0, 2)$ the sequence $(x^k)_{k \geq 0}$ generated with the algorithm CKERP converges and*

$$\lim_{k \to \infty} x^k = x^* \in [0, 1]^n \cap LSS(A; b). \tag{14}$$

Remark 2. *Some heuristic arguments sustaining the above proposed convergence result are given below:*

- *if we fix an arbitrary $k \geq 0$, then according to* (3)–(6) *we can consider in CKERP*
$$\delta^k = G \cdot P_{N(A^T)} b^{k+1} = G \cdot P_{N(A^T)}(b - y^k); \tag{15}$$
- *we know that*
$$\exists \lim_{k \to \infty} y^k = P_{N(A^T)} b; \tag{16}$$
- *from* (15) and (16) *we then get*
$$\exists \lim_{k \to \infty} \delta^k = G \cdot P_{N(A^T)} (\underbrace{b - P_{N(A^T)}(b)}_{P_{R(A)}(b)}) = 0; \tag{17}$$
- *Theorem 2 says that for CK algorithm $x^* - \delta \in LSS(A; b)$; for CKERP algorithm will then have*
$$\left\{z \in [0, 1]^n, z - \delta^k \in LSS(A; b)\right\} \overset{\substack{k \to \infty \\ \delta^k \to 0}}{\longrightarrow} \{z \in [0, 1]^n, z \in LSS(A; b)\} \tag{18}$$
i.e. CKERP would give us always a least squares solution in $[0, 1]^n$!

3. Numerical experiments

The numerical experiments have been performed with the original image shown in Fig. 3(left) which imitates an EG profile of size 30 by 30 meters. We assume the scanned area was divided into sub-regions (pixels) of size 1 by 1 meter. For scanning we used 30 positions of the transmitter, equally spaced along one borehole, and the same number of measuring points distributed along the other borehole. Thus our system matrix is $A \in \mathbb{R}^{900\times 900}$. The images reconstructed from noise-free (consistent) data with the classical Kaczmarz and KERP algorithms for 60 iterations and $x^0 = 0$ are presented in 5(a) and 5(b). The effect of the vertical smearing results from the fact that the null space components are not recovered. Using the constraining strategy described as above, we are able to get rid of the smearing effect, which is visible in Figs. 5(c) and (d). Despite the images reconstructed form noise-free data with two

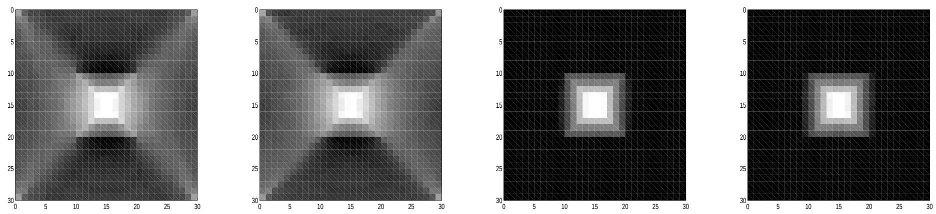

Fig. 5. Images reconstructed from noise-free (consistent) data with the algorithms (from left): (a) classical Kaczmarz (K), (b) KERP, (c) constrained Kaczmarz (CK), (d) CKERP.

different constrained algorithms (CK and CKERP) are nearly the same, the results are not the same in case of real data (noisy data). The noisy data are generated as follows: Let $g \in \mathbb{R}^m$ be a vector of a Gaussian noise with $\mu = 0$ and $\sigma^2 = 1$, then using the projection $v = P_{N(A^{\mathrm{T}})}(g)$, we have $\delta(\epsilon) = \epsilon \cdot \frac{\|b\|}{100} \cdot \frac{v}{\|v\|}$; $\quad b \stackrel{\mathrm{def}}{=} A \cdot x^{ex}, \quad b^{pert}(\epsilon) = b + \delta(\epsilon)$, where the strength of the noisy perturbations can be changed with the parameter ϵ. Using the noisy data, we obtained the results shown in Fig. 6 with the CK algorithm (top row) and the CKERP (bottom row). The CKERP algorithm is not sensitive to the noise in $N(A^{\mathrm{T}})$, thus we obtained the perfect reconstruction even for the hight values of the parameter ϵ. This motivates the usage of the CKERP instead of the CK algorithm. The convergence of the CKERP algorithm is quite satisfactory, which is illustrated in Fig. 7.

Conclusions. Our considerations show that the constraining strategy introduced by Koltracht and Lancaster in [3] to the classical Kaczmarz algorithm also works very well with the KERP algorithm. The advantage of using the constrained KERP (CKERP) algorithm over the CK algorithm is certainly this that the KERP is completely insensitive to the noisy perturbations that belong to the orthogonal complement of the range of the system matrix.

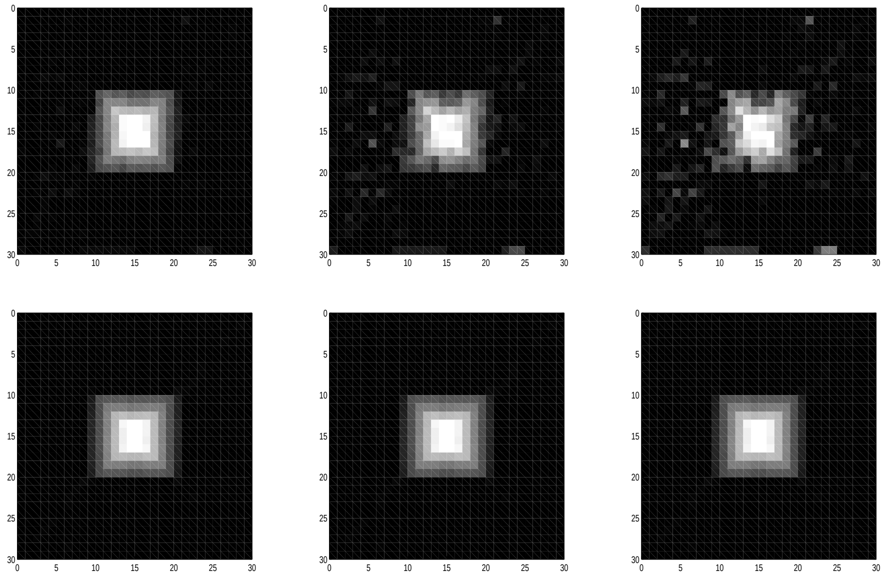

Fig. 6. Images reconstructed from noisy (inconsistent) data with the algorithms: CK (top row), CKERP (bottom row), for different values of parameter ϵ: 10 (left column), 30 (middle column), 50 (right column).

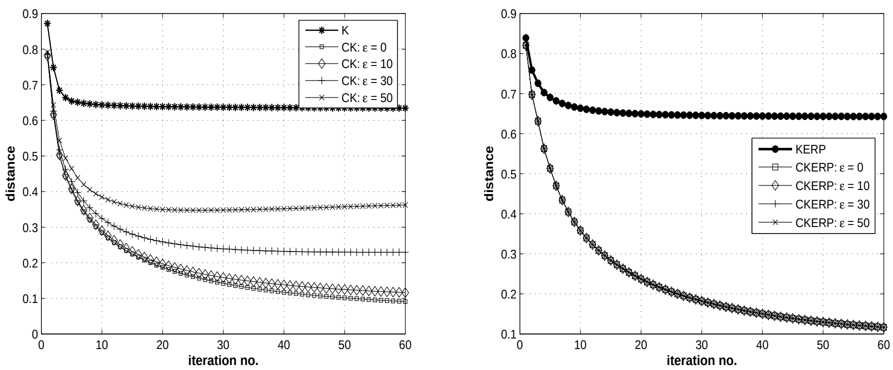

Fig. 7. Normalized Euclidean distances between the exact images (x_{exact}) and the image reconstructed with the algorithms: CK (top), CKERP (bottom).

References

[1] Björck, A., *Numerical methods for least squares problems*, SIAM Philadelphia, 1996.

[2] Elsner L., Koltracht I. and Lancaster P., *Convergence properties of ART and SOR algorithms*, Numer. Math. , **59** (1991), 91–106.

[3] Koltracht I. and Lancaster P., *Constraining strategies for linear iterative processes*, IMA Journal of Numerical Analysis, **10** (1990), 555–567.

[4] Koltracht I., Lancaster P. and Smith D., *The structure of some matrices arising in tomography*, Linear Algebra and its Applic., **130** (1990), 193–218.

[5] Lager D. L. and Lytle R. J., *Determining a subsurface electromagnetic profile from high frequency measurements by applying reconstruction technique algorithms*, Radio Science, **12** (1977), 249–260.

[6] Popa C., *Extensions of block-projection methods with relaxation parameters to inconsistent and rank-defficient least-squares problems*, *BIT*, **38(1)** (1998), 151–176.

[7] Popa C. and Zdunek R., *Kaczmarz extended algorithm for tomographic image reconstruction from limited-data*, Math. and Computers in Simulation, **65** (2004), 579–598.

[8] Pralat A. and Zdunek R., *Electromagnetic Geotomography – Selection of Measuring Freqency*, IEEE Sensors Journal, **5** (2005), 242–250.